Membrane and Water Treatment, *Vol. 10, No. 6 (2019) 431-440*
DOI: https://doi.org/10.12989/mwt.2019.10.6.431

Phenol removal by tailor-made polyamide-fly ash composite membrane: Modeling and optimization

Vandana Gupta[a] and Anandkumar J.*

Department of Chemical Engineering, National Institute of Technology, Raipur, G.E. Road, Raipur, Chhattisgarh 492010, India

(Received May 24, 2018, Revised February 23, 2019, Accepted October 5, 2019)

Abstract. A novel composite membrane was synthesized using crosslinked polyamide and fly ash ceramic substrate for phenol removal. Glutaraldehyde was used as crosslinker. Characterization shows that synthesized membrane possesses good permeability (0.184 $l.m^{-2}.h^{-1}.kPa^{-1}$), MWCO (1.7 kDa), average pore size (1.08 nm) and good chemical stability. RSM was adopted for phenol removal studies. Box-Behnken-Design using quadratic model was chosen for three operating parameters (feed phenol concentration, pH and applied pressure) against two responses (phenol removal, flux). ANOVA shows that model is statistically valid with high coefficient of determination (R^2) value for flux (0.9897) and phenol removal (0.9302). The optimum conditions are obtained as pH 2, 46 $mg.l^{-1}$ (feed phenol concentration) and 483 kPa (applied pressure) with 92.3% phenol removal and 9.2 $l.m^{-2}.h^{-1}$ flux. Data validation with deviation of 4% confirms the suitability of model. Obtained results reveal that prepared composite membrane can efficiently separate phenol from aqueous solution.

Keywords: ceramic substrate; composite membrane; phenol removal; polyamide 66; RSM

1. Introduction

Industrial effluent contains certain organic compounds which are very hazardous to environment as well as human health. Removal of organic toxic compounds from effluent is a major concern of modern era. Effluent of specific industries such as coke-oven, pesticides, petrochemicals, printing, pharmaceutical and dye contains phenol and its derivatives which are highly toxic in nature (Mukharjee *et al.* 2016, Al-Obaidi *et al.* 2017). Removal of phenol and its derivatives from discharge stream is essential before disposing into the environment. Phenol can be removed by many conventional techniques such as adsorption, extraction, chemical and UV oxidation, bio-logical treatment etc. However, these conventional techniques are having certain disadvantages such as high cost, low efficiency, high energy consumption and difficulties in recycling of chemical agent (Mixa *et al.* 2008, Zeng *et al.* 2008). Membrane separation became an emerging technique due to its high removal efficiency, economical cost and fast processing (Baubakri *et al.* 2014). However, limited literatures are reported for phenol removal using membrane techniques such as microfiltration, ultrafiltration, nano-filtration and reverse osmosis (Gonzalez-Munoz *et al.* 2003, Zeng *et al.* 2008, Zagklis *et al.* 2015, Hanafi *et al.* 2016, Jiang *et al.* 2016, Liu *et al.* 2016). Separation efficiency of membrane can be improved/altered by modifying its morphological properties. Selection of membrane precursors for its fabrication is an important factor which strongly influences the separation efficiency. In this study, polyamide 66 (PA) is chosen due to its good efficiency towards phenol removal (Reinard *et al.* 1986, Murthy and Gupta 1998, Hofman *et al.* 1997, Basu *et al.* 2017). Most of the PA composite membranes (CM) are prepared by either interfacial polymerization of meta phenylenediamine (MPD) and trimesoylchoride (TMC) or electrospinning method using polymeric support (Sridhar *et al.* 2006, Lee *et al.*2008, Wei *et al.* 2011, Al-Hobaib *et al.* 2015, Lin *et al.* 2016). Synthesis of CM using pure PA is a challenging task because it forms a soft layer on substrate surface which may partially or fully displace when it comes into the contact of aqueous media or other solvent. PA has high tendency to absorb the moisture and easily affected by strong acids as well as oxidizing agents. PA can also be dissolved by phenol and therefore, to improve the properties of PA, it is obligatory to incorporate the suitable crosslinking agent which may significantly improves the physical properties of PA membrane (Huang *et al.* 2002, Lin *et al.* 2016). PA is generally crosslinked by radiation of infrared rays and heating (Sridhar *et al.* 2006, Liesen *et al.* 2016). But, only few literatures have been reported for chemically crosslinked PA membrane. In this work PA is chemically crosslinked by glutaraldehyde to make a stable active layer on ceramic substrate.

Mostly, evaluation of membrane separation performance is carried out by conventional method of experiments. Conventional methods generally follow the variation of some parameter while keeping one parameter constant. This methodology of experiments takes huge number of runs which is time consuming, complicated, expensive and could not focus on interaction between dominating parameters

*Corresponding author, Ph.D., Assistant Professor
E-mail: anandj.che@nitrr.ac.in
[a] Ph.D. Student
E-mail: guptavandana_chem@yahoo.co.in

ISSN: 2005-8624 (Print), 2092-7037 (Online)

(Baubakri *et al.* 2014). Nowadays, researchers are focusing on response surface methodologies (RSM) which give appropriate results within reduced time span for experiments so that more time will be available for novel and effective research. Application of RSM provides design of experiment with limited number of runs and effect of interaction between process parameters. RSM contains collection of statistical model which provides the optimization of process parameter to have a good response. Data validation between experimental and predicted value can also be achieved by RSM which gives the suitability of selected model (Baubakri *et al.* 2014, Irani *et al.* 2015, Seres *et al.* 2016).

The aim of this work is to synthesize a crosslinked PA coated fly ash supported CM for phenol removal. The phenol removal experiments were designed by RSM using Box-Behnken Design (BBD) and quadratic model. Fitness of selected model was analyzed through analysis of variance (ANOVA). Influence of operating parameters such as feed concentration, feed pH and applied pressure on phenol removal efficiency is evaluated. Optimization of operational parameters is also performed to obtain the good phenol removal and permeate flux.

2. Materials and method

Polyamide 66 was procured from Sigma-Aldrich Co., Mumbai, India. Formic acid (85%), glutaraldehyde (25%), kaolin, boric acid, sodium metasilicate, sodium carbonate and poly(ethylene glycol) (MW: 1500, 4000, 6000, 10,000 and 20,000) were obtained from Merck (India) Pvt. Ltd. Mumbai. Phenol was purchased from Merck (India) Pvt. Ltd. Mumbai. HPLC grade acetonitrile and water was purchased from Fisher-Scientific, UK Ltd. Fuller clay was procured from local supplier and double distilled water was used as solvent. Fly ash was collected from National thermal power corporation (NTPC), Korba, India.

2.1 Composite membrane preparation

2.1.1 Preparation of ceramic substrate

Ceramic substrate was prepared in laboratory by using predefined composition of fly ash (72 wt%), fuller clay (8 wt%) and additives such as kaolin (15 wt%), boric acid (1.25 wt%), sodium metasilicate (1.25 wt%) and sodium carbonate (2.5 wt%). Homogenous mixture of ingredients was casted into a 5× 0.5 cm (diameter × thickness) disc using hydraulic press. Thereafter casted disc was dried in hot air oven at 105°C followed by sintering at 800°C temperature for 12 h. Then synthesized ceramic substrate was subjected to the coating process using polymeric solution to obtain composite membrane.

2.1.2 Preparation of coating solution

14% (by weight) PA was dissolved in formic acid at ambient temperature and stirred continuously to obtain homogenous solution. Then a predefined (1 wt%) quantity of glutaraldehyde was added as crosslinking agent in PA solution. Thereafter enough quantity of crosslinked PA solution (XPAG) was coated on the surface of ceramic substrate using glass rod. Coated substrate was allowed for overnight drying at ambient temperature (28 °C) (Jasni *et al.* 2016, Yanilmaz *et al.* 2017). Then, kept for heat curing at 120-150 °C temperature for 1 min to have complete cross-linking of polymeric layer (Huang *et al.* 2002).

2.2. Membrane characterization

2.2.1 Degree of crosslinking, swelling study and chemical stability

Solvent extraction method was used to determine the degree of crosslinking of synthesized XPAG CM. A small piece of membrane was wrapped with filter paper and kept in solvent (1M formic acid) at ambient temperature. Solvent was replaced with fresh solvent after each 15 h till the polymer exhibited no solubility in solvent (Kumar *et al.* 2015, Rudra *et al.* 2015). When the polymer became insoluble in solvent, then sample was dried and weighed. The degree of crosslinking is calculated in terms of gel fraction using following Eqs

$$W = W_f/W_i \times 100 \quad (1)$$

where W_i and W_f is initial and final dry weight (g) of membrane.

The degree of swelling and chemical stability of membrane was calculated in terms of mass uptake and weight loss, respectively using gravimetric method. Known mass of membrane samples was immersed in neutral, highly acidic (pH≈2) and highly alkaline (pH≈13) solution for 48 h. Thereafter, samples were taken out and wiped gently by tissue paper. Swollen weight of sample was measured and degree of swelling was calculated by Eq. (2). Chemical stability was checked by analyzing the permeability and dry weight of membrane before and after immersing the membrane in acid and basic solution.

$$S_d = \frac{W_s - W_d}{W_d} \times 100 \quad (2)$$

2.2.2 Compaction, hydraulic permeability and molecular weight cut-off (MWCO) study

A dead-end filtration set-up (Fig. 1) was used for conducting the permeation experiments. Nitrogen gas cylinder was used to apply the pressure and regulated by outlet valve connected with cylinder.

The rigid porous structure and size of membrane is essential to have a steady hydraulic characteristic. Compaction study provides rigidness in pore structure. This study was conducted by filling the filtration setup with 250 ml of double distilled water operated at 483 kPa pressure. Pure water flux was obtained for each 10 min interval. Hydraulic permeability was calculated by plotting flux against pressure. Flux through membrane was calculated for different applied pressure (69-483 kPa). The slope of graph between flux and pressure gives the permeability ($l.m^{-2}.h^{-1}.kPa^{-1}$). Flux through the membrane can be calculated by the following Eqs

$$\text{Flux (J)} = \frac{V}{A.t} \quad (3)$$

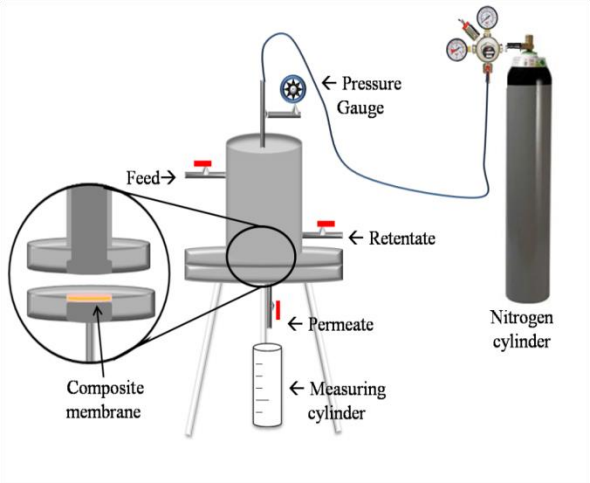

Fig. 1 Schematic of dead-end filtration setup

where J is in $l.m^{-2}.h^{-1}$), V,A and t are permeate volume (l), membrane area (m^2) and time (h), respectively.

MWCO study of CM was carried out with different molecular weights (0.2, 0.4, 0.6, 1.5, 6, 10 and 20 kDa) of polyethylene glycol (PEG). PEG test solutions were prepared with double distilled water. Test conditions (operating pressure 207 kPa and 10 $g.l^{-1}$ solute concentrations) were kept constant throughout this study. The retention of PEG (%R) was determined by the following Eq

$$\% R = 1 - \frac{C_p}{C_f} \times 100 \quad (4)$$

where, R, C_p and C_f represents solute rejection (%), permeate and feed concentration, respectively. Solute concentration was measured by Abbe Refractometer (Model: 135005, Make: Contech, India). MWCO values were obtained from PEG retention versus molecular weight curve corresponding to R = 90%. The average pore radius of membrane can be measured by Guerout-Elford-Ferry relation given in the Eq. (5).

$$r_m = 16.73 \times 10^{-10} M_w^{0.557} \quad (5)$$

where r_m and M_w is the pore radius (cm) and MWCO of membrane (Da).

2.2.3 Contact angle, SEM and FTIR analysis

Hydrophilic and hydrophobic nature of the active top layer was analyzed by contact angle analyzer (Model: Phoenix 300, Make: SEO, Korea). Sessile drop technique was used to find the contact angle between water droplet and active layer. 13 µl of double distilled water was gently dropped on different spots of active layer. Images of contact angle were obtained by using image processing software (surfaceware8).

Morphological structure of active layer was investigated by using scanning electron microscope (SEM) analysis (Model EV018: Make: Carl Zeiss, Germany). Fourier transfer infrared spectroscopy (Model: Alfa, Make:Bruker, Germany) analysis was carried-out to find the presence of different functional groups present in the active layer.

2.3 Application of RSM for phenol removal

Phenol removal studies were performed to investigate the separation efficiency of XPAG CM. Concentration of feed and permeate phenol was analyzed by using high performance liquid chromatography (HPLC) (Model: 1260, Make: Agilent technology, US). HPLC grade acetonitrile (70%) and water (30%) was used as solvent to find the phenol concentration by UV detector at 280 nm in isocratic mode with the retention time of 1.6 min.

RSM tool was employed to optimize the operating parameters of phenol removal. Responses were obtained from Box-Behnken experimental Design (BBD) with 3 factors at 3 levels and 17 runs of experiment (Irani *et al.* 2015; Seres *et al.* 2016). Experiments were conducted as per the design of experiment (DOE) developed by RSM (Table 1).The input factors include operating parameters which are feed phenol concentration, feed pH and applied pressure. The influence of input factor was investigated for two responses such as percentage removal of phenol and phenol permeate flux. RSM helps in effective parameter optimization with less number of experiments and interaction between parameters (Baubakri *et al.* 2014). Quadratic model with second order was best fitted to describe the responses (Eq. (6)).

$$Y = b_0 + b_1X_1 + b_2X_2 + b_3X_3 + b_4X_1X_2 + b_5X_2X_3 + b_6X_3X_1 + b_7X_1^2 + b_8X_2^2 + b_9X_3^2 \quad (6)$$

where Y is the response, b_0 is an intercept, X_1, X_2 and X_3 are the input factors and X_1^2, X_2^2 and X_3^2 are their quadratic terms, b_1- b_9 is the regression coefficient, interactions of input factors are represented by X_1X_2, $X_2X_3$and X_3X_1. The quality of fit for selected model can be estimated by R^2 value and model's p-value (Seres *et al.* 2016). If p-value < 0.05 then corresponding variable is considered to be more significant. Significance of selected model for input parameter and response was evaluated by ANOVA using Design-Expert 10 software. Residual plot was plotted to observe the influence and interaction of operating parameters on both responses. Residual plot is obtained with 2 operating parameters when 3rd factor kept at mean value with 95% confidence limit.

3. Result and discussion

3.1 Membrane characterization

3.1.1 Degree of crosslinking

In this work, degree of cross-linking explains about addition of glutaraldehyde as crosslinking agent with PA. Degree of crosslinking in XPAG was calculated as 93% by using Eq. (1). Crosslinking of PA takes place by the substitutions of amino groups present in the PA backbone with two –CHO groups of glutaraldehyde (Huang *et al.* 2002). This interaction limits the dissolution of crosslinked polyamide layer in 1 M formic acid whereas pure PA layer easily dissolves in the same solvent. The interaction of PA with glutaraldehyde during the crosslinking is shown in Scheme 1 (Huang *et al.* 2002, Sridhar *et al.* 2006).

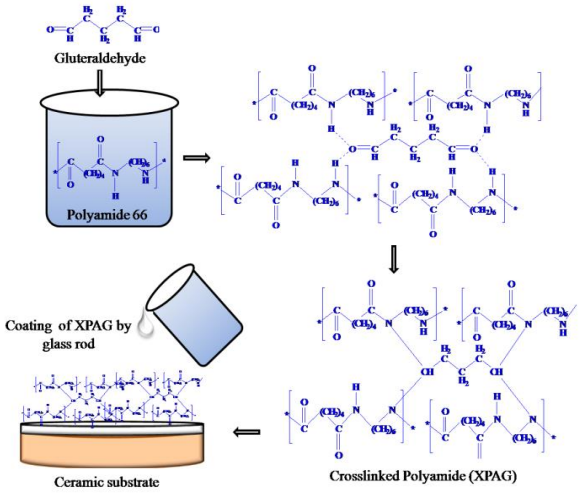

Scheme 1 Pictorial presentation of composite membrane fabrication

Table 1 Experimental design for BBD with 3 input factors

Input factors/variable	Symbol	Factor level		
		-1	0	+1
Initial feed concentration ($mg.l^{-1}$)	X_1	10	105	200
Feed Ph	X_2	2	7	12
Applied pressure (kPa)	X_3	69	276	483
Response				
Flux ($l.m^{-2}.h^{-1}$)				
Phenol removal (%)				

3.1.2 FTIR analysis

FTIR spectrum of pure and crosslinked PA is shown in Fig. 2. In pure PA, no peaks are visible in between 2500-1900 cm^{-1} whereas vibration of peak from 2350-1960 cm^{-1} is clearly perceptible in XPAG spectrum. This vibrational peak is due to multiple bonded nitrogen compound resulted by crosslinking of PA with glutaraldehyde (Coates 2000). The assignment of probable functional group according to the wave-number (cm^{-1}) is given in Table 2 (Reinhard *et al.* 1986, Belfer *et al.* 1998, Charles *et al.* 2009, Porubska *et al.* 2012, Mazry *et al.* 2012, Kann *et al.* 2014).

3.1.3 Swelling and chemical stability study

Degree of swelling in terms of water uptake capacity was calculated by Eq. (1). Swelling of PA and XPAG membrane was found to be 75% and 28.21%, respectively. High swelling of PA membrane is due to the formation of weak bond between water molecule and polyamide amino group. Hence, polyamide layer is less stable on ceramic substrate (Howe 2010). Addition of glutaraldehyde in polyamide reduces the number of amino groups which reduces swelling and makes more stable layer on substrate. The chemical stability of XPAG CM was found to be superior in highly acidic, neutral and alkaline media with negligible weight loss (< 0.5%). The changes in permeation flux through XPAG CM before and after the chemical immersion were also insignificant (Murthy and Gupta 1998).

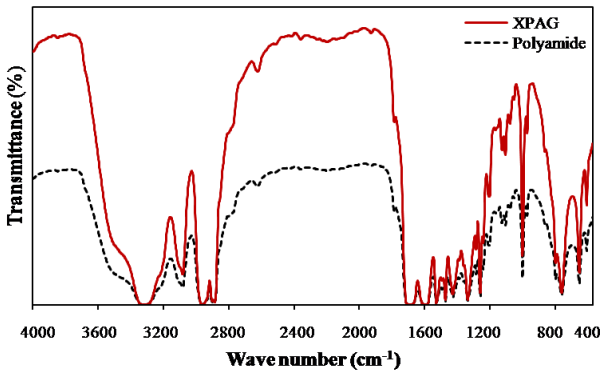

Fig. 2 FTIR spectrum of polyamide and cross-linked polyamide layer

Table 2 FTIR spectra and assignment of PA and XPAG top layer

Polyamide layer		Crosslinked polyamide layer	
Wave number (cm^{-1})	*Assignment*	*Wave number (cm^{-1})*	*Assignment*
3298	NH stretching	3321	NH stretching
3059	Aromatic C-H stretching	3059	Aromatic C-H stretching
2935	CH_2 asymmetric stretching	2944	CH_2 asymmetric stretching
2859	CH_2 symmetric stretching	2859	CH_2 symmetric stretching
1625	Amide I band	1737	C=O stretching
1548	NH band	1528	NH band
1371	Amide III	1371	Amide III
1199	CH_2-NH	1199& 1181	CH_2-NH
934	C-C=O stretching	1143	CO deformation
690	NH band	1013	C-C stretching
		934	C-C=O
		907	CH_2 stretching
		728	CH_2 rocking
		690	NH band
		534	O=C-N

3.1.4 Compaction, hydraulic permeability and MWCO study

Compaction study of XPAG CM was carried out to obtain the steady state condition of pure water permeation flux (Fig. 3). It can be seen from Fig. 3 that pure water flux gradually decreases initially and reaches steady state after 220 min run. This is due to fact that during compaction pore walls become denser, closer and uniform that resulted in the reduction of flux until steady state flux was (79.42 $l.m^{-2}.h^{-1}$) achieved (Nandi *et al.* 2009). Fig. 3 also depicts the effect of applied pressure on pure water flux. Flux increases with increase in pressure which is due to the enhancement of driving force with pressure and also very tiny pores starts to permeate with increasing pressure (Vasanth *et al.* 2013). Hydraulic permeability (0.184 $l.m^{-2}.h^{-1}.kPa^{-1}$) can be obtained from the slope of graph between pressure and water flux.

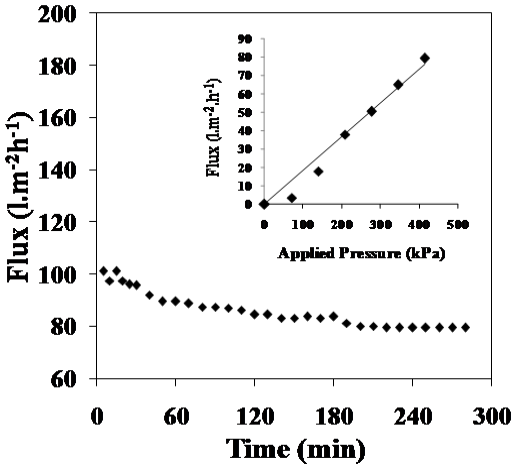

Fig. 3 Pure water flux through XPAG with varying time and applied pressure

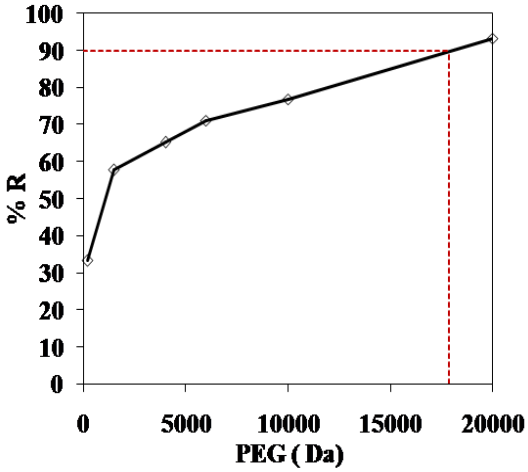

Fig. 4 MWCO study with PEG (10 g/l) at 276 kPa pressure

MWCO study was performed with different molecular weights of PEG. It can be observed from Fig. 4 that MWCO of XPAG CM is 1.78 kDa. MWCO and average pore size of membrane has a linear relation which can be expressed by Eq. (5) (Kanagaraj *et al.* 2015, Jasni *et al.* 2016). The average pore size of XPAG CM is calculated as 1.08 nm. MWCO study shows that the synthesized membrane comes under nano-filtration range.

3.1.5 Contact angle and scanning electron microscopic analysis

Contact angle of water droplet with pure PA and XPAG is shown in Fig.5. Contact angle of PA membrane and XPAG was 55.06 and 48.12, respectively. It can be seen from Fig. 5 that value of contact angle decreases when glutaraldehyde was introduced as crosslinking agent. The decrease in contact angle shows the enhancement of hydrophilic nature, increase of surface roughness and water flux (Rosa and De-pinho, 1997, Li *et al.* 2017). This result shows significant improvement in PA after crosslinking and makes it suitable for various applications.

The surface morphology of synthesized CM is shown as SEM micrograph in Fig.6. SEM image depicts that pure PA

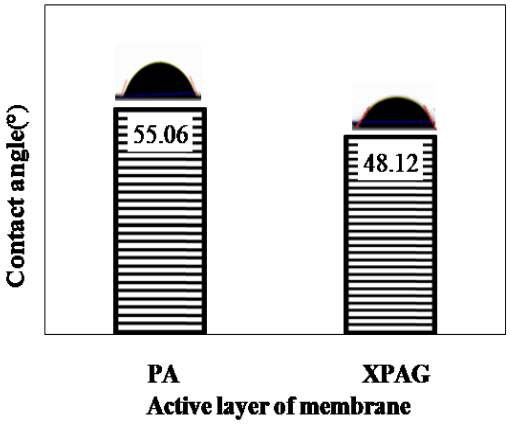

Fig. 5 Contact angle of water on PA and XPAG surface

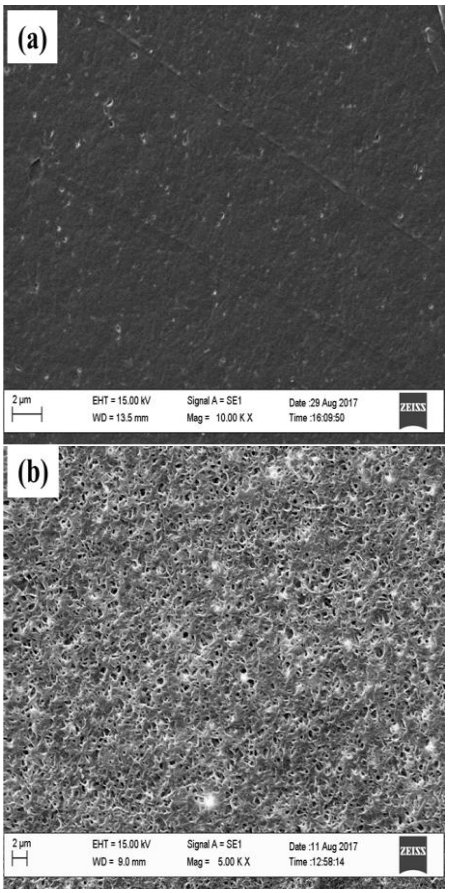

Fig. 6 SEM images of (a) PA and (b) XPAG CM

CM has less porous structure than XPAG CM which supports the data of contact angle analysis. Hence, XPAG CM has less interfacial resistance due to more porosity (Yanilmaz *et al.* 2017). SEM images also show the defect free surface for both membranes.

3.2 Evaluation of separation performance by RSM

RSM was applied to evaluate the influence of membrane process parameters such as feed phenol concentration (50-200 mg.l^{-1}), feed pH (2-12) and applied pressure (69-483 kPa) for phenol removal efficiency and permeate flux. DOE was obtained for 3 input factors and 2 responses by using

Table 3 Results for Box-Behnken design and responses in terms of % removal and permeate flux

Run	Input factors			Response	
	Concent-ration ($mg.l^{-1}$)	pH	Press-ure (kPa)	Removal (%)	Permeate Flux ($l.m^{-2}.h^{-1}$)
1	105	7	276	64.73	5.42
2	10	7	69	98.06	1.08
3	105	7	276	64.73	5.42
4	105	7	276	64.73	5.42
5	10	2	276	77.78	5.78
6	105	2	483	88.45	10.11
7	10	7	483	74.00	7.58
8	200	2	276	70.46	6.14
9	105	7	276	64.73	5.42
10	200	7	69	64.17	2.17
11	105	12	69	92.34	1.81
12	105	7	276	64.73	5.42
13	105	2	69	47.97	3.61
14	200	12	276	90.56	5.42
15	105	12	483	46.47	9.39
16	200	7	483	56.33	9.39
17	10	12	276	67.59	5.42

Table 4 ANOVA results for phenol removal (%) with BBD and quadratic model

Source	Degree of freedom	Mean square	Standard deviation	F-value	p-value	R^2	R^2_{adj}
Model	9	241.99	4.83	10.37	0.002752	0.9302	0.84
Residual	7	23.34					
Lack of fit	3	54.46					
Pure error	4	0					
Total	16						

Table 5 ANOVA of Box-Behnken quadratic model for permeate flux

Source	Degree of freedom	Mean square	Standard deviation	F-value	p-value	R^2	R^2_{adj}
Model	9	11.44	0.3919	74.48	$4.06_6 \times 10^{-}$	0.9897	0.9764
Residual	7	0.154					
Lack of fit	3	0.358					
Pure error	4	0					
Total	16						

BBD (Table 1). Seventeen runs of experiments were performed to evaluate the influence of process parameters on responses by fitting quadratic model. Phenol removal experiments were conducted in dead end filtration setup. After achieving the steady state value of flux, samples were collected for each 10 min interval and analyzed. Flux and phenol removal was calculated by Eq. (3) and (4). BBD experimental data obtained for each response at different operating condition are shown in Table 3.

3.2.1 Statistical evaluation of process parameter for phenol removal

Experiments were conducted to investigate the level of process parameter. The statistical combination and phenol removal percentage is listed in Table 3. The responses obtained were plotted against process variable and influence of variable was investigated by ANOVA (Table 4).

Coefficient of determination (R^2) for phenol removal response was found to be 93.02% which indicates that only 7% of variation can't be explained by this method (Seres *et al.* 2016). The coefficients of regression derived by BBD model are given in Eq. (7) and Eq. (8). The p-value (0.0027) reveals the significance of input factors for fitted model. Regression Eqs shows the empirical relation between phenol removal efficiency with three variables. The regression Eqs obtained in terms of coded and actual variable can be written as follow:

$$\text{Removal (\%)} = \begin{matrix} 68.73 - 2.37625.X_1 + 0.3425.X_2 - \\ 2.85375.X_3 + 5.6825.X_1.X_2 + \\ 2.94.X_1.X_3 - 21.0875.X_3.X_1 + \\ 5.3475.X_1^2 + 0.63.X_2^2 - 0.0525.X_3^2 \end{matrix} \quad (7)$$

$$\text{Removal (\%)} = \begin{matrix} 56.1181091 + 0.274447784 \times \text{Feed conc.} + 4.082901754 \times \text{Feed pH} + \\ 0.113812929 \times \text{Pressure} + \\ 0.011963158 \times \text{Feed conc.} \times \text{Feed pH} + 0.000149504 \times \text{Feed conc.} \times \\ \text{Pressure} + 0.020374396 \times \text{Feed pH} \times \text{Pressure} + 0.000592521 \times (\text{Feed conc.})^2 + 0.0252 \times (\text{Feed pH})^2 - \\ 1.22523 \times 10^{-06} (\text{Pressure})^2 \end{matrix} \quad (8)$$

3D response surface plot for Phenol removal is shown in Fig.7A-C. Fig.7A shows the influence of feed pH and feed concentration on phenol removal while keeping the pressure at 276 kPa. It is observed that the phenol removal increases with increasing pH for 200 mg phenol/l. Phenol removal increases from 70.46% to 91% with increase in pH (pH 2 to pH 12). Maximum removal of phenol is obtained at pH 12. This result reveals that feed phenol pH has strong influence on separation efficiency of XPAG. It is due to fact that at high pH, phenol exists in anionic (phenolate anion) form whereas in acidic (low) pH mostly it is in molecular form. Therefore, electrostatic repulsion occurs between negatively charged active layer (XPAG) and phenolate anion which leads to the high removal of phenol at high pH (Li *et al.* 2010, Djamila *et al.* 2016). Fig.7B shows the effect of pressure and pH on phenol removal performance. Phenol removal decreases with increasing pressure. Maximum removal of 92.34% phenol was obtained at 69 kPa pressure and pH 12. At high pressure, tiny pores also turned to permeate the phenol molecules which resulted as more phenol concentration in the permeate side (Li *et al.* 2010, Vasanth *et al.* 2013). It is observed from Fig.7C that feed

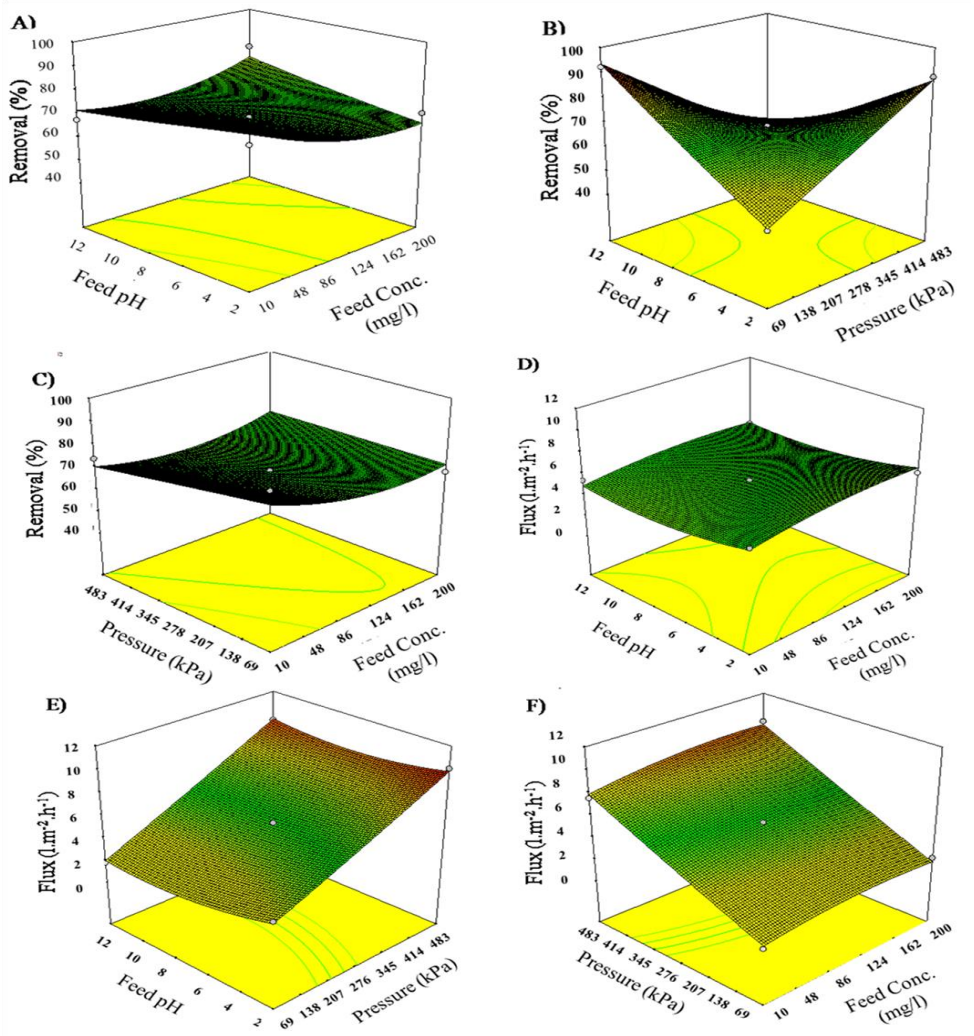

Fig. 7 Response surface plots of phenol removal and permeate flux as function of operating factors. (A) Phenol removal (%R) vs feed pH and feed concentration ($mg.l^{-1}$); (B) Phenol removal (%R) vs feed pH and pressure (kPa); (C) Phenol removal (%R) vs pressure (kPa) and feed concentration ($mg.l^{-1}$); (D) permeate flux vs feed pH and feed concentration ($mg.l^{-1}$); (E) Permeate flux vs feed pH and pressure (kPa); (F) permeate flux vs pressure (kPa) and feed concentration ($mg.l^{-1}$)

concentration has slight influence on phenol removal. Phenol removal slightly decreases with increasing concentration and the maximum removal was obtained as 74% at 483 kPa for 10 $mg.l^{-1}$. Increase in feed concentration increases the molecular friction of phenol molecule along with the membrane surface and thus increases the permeate phenol concentration (Porubska *et al.* 2012).

3.2.2 Statistical evaluation of process parameter for permeate flux

Experiments were conducted as per DOE and assessed statistically with similar factors applied for phenol removal. Influence of process parameters on permeate flux was tested by ANOVA. The outcomes of statistical validation are reported in Table 5 and the responses are shown in Fig. 7 D-F.

The effectiveness of model can be estimated by some estimators such as p-value and R^2 etc. (Baubakri *et al.* 2014, Irani *et al.* 2015). When p-value<0.05, then the corresponding variable is more significant. The obtained p-value of 4.06×10^{-06} shows that the model is highly significant for this response. The obtained coefficient of determination is 0.9897 which implies 98.97% of data deviation hence it can be expressed by given model. Therefore, regression model is statistically significant.

The empirical relationship between process parameter and permeate flux in terms of coded and actual variable can be represented as:

$$\text{Flux}= 5.415162 + 0.406137.X_1 - 0.45126.X_2 + 3.474729.X_3 - 0.09025.X_1.X_2 + 0.180505.X_1.X_3 + 0.270758.X_3.X_1 - 0.45126.X_1^2 + 0.722022.X_2^2 - 0.090253.X_3^2 \quad (9)$$

$$\text{Flux} = 2.621185 + 0.013572 \times \text{Feed conc.} - 0.54684 \times \text{Feed pH} + 0.012828 \times \text{Pressure} - 0.00019 \times \text{Feed conc.} \times \text{Feed pH} + 9.18 \times10^{-06}\times \text{Feed conc.} \times \text{Pressure} + 0.000262\times \text{Feed pH} \times \text{Pressure} - 5 \times10^{-05}\times (\text{Feed conc.})^2 + 0.028881\times (\text{Feed pH})^2 - 2.11\times10^{-06} (\text{Pressure})^2 \quad (10)$$

The influence of pH and concentration on permeate flux is shown in Fig. 7D. It was found that influence of pH and feed concentration on flux was negligible with less than 1 $l.m^{-2}.h^{-1}$ difference. Effect of pressure on flux is shown in Fig.7E. Pressure has notable influence on permeate flux. The flux increases with increasing pressure from 1.81 to 9.39 $l.m^{-2}.h^{-1}$ for pressure of 69 and 483 kPa during feed pH had negligible effect. This is due to the fact that at high pressure very tiny pores which were impermeable at low pressure also became permeable and hence flux increases (Vasanth *et al.* 2013). Effect of concentration with pressure and flux is shown in Fig.7F. It can be seen from the Fig. 7F that feed concentration has negligible effect on permeate flux and maximum flux was obtained as 9.39 $l.m^{-2}.h^{-1}$ for 200 $mg.l^{-1}$. The negligible changes in the membrane flux due to the pH and feed concentration change might be related to the transport mechanism. Since the applied pressure is acting as main driving force of XPAG CM than any other driving forces, pressure has only the greatest influence on permeate flux.

The operating parameters were optimized to get significant removal with good permeate flux using Designexpert10 software. Optimizing software scans the basic terms of model such as response surface, main effect and interaction between the input factors. This provides best suitable conditions for the process and desirability function (Baubaklri *et al.* 2014).

3.2.3 Data optimization and validation

Optimum conditions obtained by software for feed pH, concentration and applied pressure are pH 2, 46 $mg.l^{-1}$ and 483kPa, respectively. The phenol removal (92.3%) and flux (9.2 $l.m^{-2}.h^{-1}$) was predicted with optimum values. Desirability of model was estimated by analyzing the closeness of regression (0.954) with ideal response. Data validation for predictive model and optimized value was carried out by performing the experiments under optimized condition. The experimental results obtained for phenol removal and flux are 90% and 8.9 $l.m^{-2}.h^{-1}$, respectively whereas 92.3 % phenol removal and 9.2 $l.m^{-2}.h^{-1}$ flux was predicted by the model. These outcomes show 2.5% and 3.3% deviation between experimental and predicted value for phenol removal and flux, respectively. Results obtained from the experimental validation are within the predicted value of 97%. Hence, results show the suitability of the developed model and this may be valid for optimal value of variable parameter.

3.3 Superiority of XPAG CM for phenol separation

Synthesized XPAG CM possesses high phenol removal (90%) efficiency than recently reported membranes in the literature. For instance 71.7%, 75% and 58% of phenol removal is reported by Khazaali *et al*. (2017), Arsuaga *et al*. (2011) and Kargari *et al*. (2015), respectively using polyamide based thin film composite membrane. Moreover, simple glass rod method was adopted for synthesis of XPAG CM. Therefore, synthesized XPAG CM is superior than literature reported membranes in terms of its phenol removal efficiency and fabrication method.

4. Conclusion

XPAG CM was synthesized for separation of phenol from aqueous solution. XPAG CM exhibits high chemical stability and less swelling degree as compared to pure PA membrane. MWCO study confirms the nanoporous structure of XPAG composite membrane. Crosslinking with glutaraldehyde increases the hydrophilic nature of CM which makes it more suitable for phenol-water separation. SEM micrograph ensures that membrane surface is uniform and defect free. ANOVA result demonstrates that BBD with quadratic model has more significance with high R^2 value for phenol removal and permeate flux. The optimum response results are obtained as 92.3 % phenol removal and 9.2 $l.m^{-2}.h^{-1}$ flux at pH 2, 46 $mg.l^{-1}$ feed phenol concentration and 483kPa applied pressure. Data validation between predicted values and experimental values shows less than 4% deviation which confirms the suitability of developed model. Experimental data of phenol removal demonstrates that synthesized XPAG CM has high separation efficiency for phenol removal and RSM could be used a best tool for optimization of membrane process parameters.

Acknowledgement

This work is supported by a grant from Department of Science and Technology (SERB), New Delhi, Government of India, under the scheme of Early Career Research Award (ECR/2016/000435 dated 09-09-2016).

References

Al-Obaidi, M.A., Kara-Zaïtria, C. and Mujtaba, I.M. (2017), "Removal of phenol from wastewater using spiral-wound reverse osmosis process: Model development based on experiment and simulation", *J. Water Process Eng.*, **18**, 20-28. http://dx.doi.org/10.1016/j.jwpe.2017.05.005.

Al-Hobaib, A.S., El Ghoul, J., El Mir, L. (2015), "Synthesis and characterization of ployamide thin film nanocomposite membrane containing ZnO nanoparticle", *Membr. Water. Treat.*, **6**(4), 309-321. https://doi.org/10.12989/mwt.2015. 6.4.309.

Arsuaga, J.M., Sotto, A., López-Munoz, M.J., Braeken, L. (2011), "Influence of type and position of functional groups of phenolic compounds on NF/RO performance", *J. Membr. Sci.*, **372**, 380-386. https://doi.org/10.1016/j. memsci.2011.02.020.

Basu, S. and Balakrishnan, M. (2017), "Polyamide thin film composite membranes containing ZIF-8 for the separation of pharmaceutical compounds from aqueous streams", *Sep. Purif. Technol.*, **179**, 118-125. http://dx.doi.org/10.1016/ j.seppur.2017.01.061.

Belfer, S., Purinson, Y. and Kedem, O. (1998), "Surface modification of commercial polyamide reverse osmosis membranes by radical grafting: An ATR-FTIR study", *Acta. Polym.*, **49**, 574-582. https://doi.org/10.1002/(SICI)1521-4044(199810)49:10/11<574::AID-APOL57 4>3.0.CO;2-0.

Boubakri, A., Hafiane, A. and Bouguecha, S.A.T. (2014), "Application of response surface methodology for modeling and optimization of membrane distillation desalination process", *J. Ind. Eng. Chem.*, **20**, 3163-3169. http://dx.doi.org/10.1016/j.jiec.2013.11.060.

Charles, J., Ramkumaar, G.R., Szhagiri, S. and Gunasekaran, S.

(2009), "FTIR and Thermal Studies on Nylon-66 and 30% Glass Fibre Reinforced Nylon-66", *e-J chem. coden ecjhao,* **6**(1), 23-33. http://dx.doi.org/10.1155/2009/909 017.

Coates, J. (2000) *Interpretation of Infrared Spectra, A Practical Approach Encyclopedia of Analytical Chemistry,* R.A. Meyers (Ed.) John Wiley and Sons Ltd, Chichester, USA. 10815-10837.

Djamila, G., Djamel, A. and Nedjla, A. (2016), "Selective adsorption of 2-nitrophenol, phenol, hydroquinone on Poly (Vinyl Alcohol) crosslinked glutaraldehyde-β-cyclodextrin polymer membrane", *J. Polym. Biopolym. Phys. Chem.*, **4**(1), 7-15. https://doi.org/10.12691/jpbpc-4-1-2.

González-Muñoz, M.J., Luque, S., Álvarez, J.R. and Coca, J. (2003), "Recovery of phenol from aqueous solutions using hollow fibre contactors", *J. Membr. Sci.*, **213**, 181-193. https://doi.org/10.1016/S0376-7388(02)00526-4.

Hanafi, Y., Loulergue, P., Ababou-Girard, S., Meriadec, C., Rabiller-baudry, M., Baddari, K. and Szymczyk, A. (2016), "Electrokinetic analysis of PES/PVP membranes aged by sodium hypochlorite solutions at different pH", *J. Membr. Sci.*, **501**, 24-32. http://dx.doi.org/10.1016/j.mem sci.2015.11.041.

Hemmati, M., Nazari, N., Hemmati, A. and Shirazian, S. (2015) "Phenol removal from wastewater by means of nanoporous membrane contactors", *J. Ind. Eng. Chem.*, **21**, 1410-1416. http://dx.doi.org/10.1016/j.jiec.2014.06.015.

Hofman, J.A.M.H., Beerendonk, E.F., Folmer, H.C. and Kruithoff, J.C. (1997) "Removal of pesticides and other micropollutants with celluloseacetate, polyamide and ultra-low pressure reverse osmosis membranes", *Desal*., **113**, 209-214. PII S0011-9164(97)00131-8.

Howe, B. (2010), UL Prospector Dry vs. Conditioned Polyamide Nylon Explained. Prospector. Prospector knowledge center. https://knowledge.ulprospector.com/1489/pe-dry-vs-conditioned-polyamide-nylon.

Huang, Z.H., McDonald, W.E., Wright, S.C. and Taylor, A.C. (2002) "Cross linked polyamide", US Patent US 6,399,714 B1. https://patents.google.com/patent/US6399714B1/en.

Irani, M., Rad, L.R., Pourahmad, H. and Haririan, I. (2015), "Optimization of the combined adsorption/photo-Fenton method for the simultaneous removal of phenol and paracetamol in a binary system", *Microporous Mesoporous Mater.*, **206**, 1-7. http://dx.doi.org/10.1016 /j.micromeso.2014.12.009.

Jasni, M.J., Sathishkumar, P., Sornambikai, S., Yusoff, A.R.M., Ameen, F., Buang, N.A., Kadir, M.R.A. and Yusop, Z. (2016). "Fabrication, characterization and application of laccase-nylon 6,6/Fe^{3+} composite nanofibrous membrane for 3,30-dimethoxybenzidine detoxification", *Bioprocess Biosyst. Eng.*, **40**(2), 191-200, https://dx.doi.org/10. 1007/s00449-016-1686-6.

Jiang, H., Qu, Z., Li, Y., Huang, J., Chen, R. and Xing, W. (2016), "One-step semi-continuous cyclohexanone production via hydrogenation of phenol in a submerged ceramic membrane reactor", *Chem. Eng. J.*, **284**, 724-732. https://doi.org/10.1016/j.cej.2015.09.037.

Kanagaraj, P., Nagendran, A., Rana, D., Matsuura, T. and Neelakandan, S. (2015), "Separation of macromolecular proteins and rejection of toxic heavy metal ions by PEI/cSMM blend UF membranes". *Int. J. Biol. Macromol.*, **72**, 223-229. http://dx.doi.org/doi:10.1016/j.ijbiomac.201 4.08.018.

Kann, Y., Shurgalin, M. and Krishnaswamy, R.K. (2014) "FTIR spectroscopy for analysis of crystallinity of poly(3-hydroxybutyrate-co-4 -hydroxybutyrate) polymers and its utilization in evaluation of aging, orientation and composition", *Polym. Test.*, **40**, 218-224. http://dx.doi.org/10.1016/j.polymertesting.2014.09.009.

Kargari, A., Mohammadi, S. (2015), "Evaluation of phenol removal from aqueous solutions by UV, RO, and UV/RO hybrid systems", *Desalin. Water. Treat.*, **54**(6), 1-9. http://dx.doi.org/10.1080/19443994.2014.891077.

Khazaali, F., Kargari, A. (2017), "Treatment of Phenolic Wastewaters by a Domestic Low-Pressure Reverse Osmosis System", *J. Membr. Sci. Res.*, **3**, 22-28. https://dx.doi.org/10.22079/JMSR.2017.23344.

Kumar, V., Kumar, P., Nandy, A. and Kundu, P.P. (2015), "Crosslinked inter penetrating network of sulfonated styrene and sulfonated PVdF-co-HFP as electrolytic membrane in single chambered Microbial Fuel Cell", *RSC adv.*, **5**, 30758-30767. https://doi.org/10.1039/C5RA034 11F.

Lee, H.S., Im, S.J., Kim, J.H., Kim, H.J., Kim, J.P. and Min, B.R. (2008), "Polyamide thin-film nanofiltration membranes containing TiO_2 nanoparticles", *Desal.*, **219**, 48-56. https://doi.org/10.1016/j.desal.2007.06.003.

Li, H., Zhang, H., Qin, X. and Sh, W. (2017), "Improved separation and antifouling properties of thin-film composite nanofiltration membrane by the incorporation of cGO", *Appl. Surf. Sci.*, **407**, 260-275. http://dx.doi.org/10.1016/j.apsusc.2017.02.204.

Li, Y., Wei, J., Wanga, C. and Wang, W. (2010), "Comparison of phenol removal in synthetic wastewater by NF or RO membranes". *Desalin. Water. Treat.*, **22**, 211-219. http://dx.doi.org/10.5004/dwt.2010.1787.

Lin, S., Huang, H., Zeng, Y., Zhang, L. and Hou, L. (2016), "Facile surface modification by aldehydes to enhance chlorine resistance of polyamide thin film composite membranes", *J. Membr. Sci.*, **518**, 40-49. http://dx.doi.org/10.1016/j.memsci.2016.06.032.

Liu, Y., Meng, M., Yao, J., Da, Z., Feng, Y., Yan, Y. and Li, C. (2016), "Selective separation of phenol from salicylic acid effluent over molecularly imprinted polystyrene nanospheres composite alumina membranes", *Chem. Eng. J.*, **286**, 622-631. https://doi.org/10.1016/j.cej.2015.10.063.

Mazry, C.E., Correc, O. and Colin, X. (2012), "A new kinetic model for predicting polyamide 6-6 hydrolysis and its mechanical embrittlement", *J. Polym. Degrad. Stab.*, **97**, 1049-1059. https://hal.archives-ouvertes.fr/hal-01082759.

Mixa, A. and Staudt, C. (2008), "Membrane-based separation of phenol/water mixtures using ionically and covalently cross-linked ethylene-methacrylic acid copolymers", *Int. J. Cheme.*, **2008**, 1-12. http://dx.doi.*org*/10.1155/2008/319 392.

Mukherjee, R. and De, S. (2016), "Novel carbon-nanoparticle polysulfone hollow fiber mixed matrix ultrafiltration membrane: adsorptive removal of benzene, phenol and toluene from aqueous solution", *Sep. Purif. Technol*, **157**, 229-240. http://dx.doi.org/10.1016/j.seppur.2015.11.015.

Murthy, Z.V.P. and Gupta, S.K. (1998) "Thin film composite polyamide membrane parameters estimation for phenol-water system by reverse osmosis", *Sep. Sci. Technol.*, **33**(16), 2541-2557. http://dx.doi.org/10.1080/014963998 08545318.

Nandi, B.K., Uppaluri, R. and Purkait, M.K. (2009), "Effect of dip coating parameters on the morphology and transport properties of cellulose acetate-ceramic composite membrane", *J. Membr. Sci.*, **330**, 246-258. https://doi.org/10.1016/j.memsci.2008.12.071.

Porubská, M., Szöllos, O., Kónová, A., Janigová, I., Jasková, M., Jomová, K. and Chodák, I. (2012) "FTIR spectroscopy study of polyamide-6 irradiated by electron and proton beams", *Polym. Degrad. Stability*, **97**, 523-531. https://dx.doi.org/10.1016/j.polymdegradstab.2012.01.017.

Reinhard, M.R., Goodman, N.L., McCarty, P.L. and Argo, D.G. (1986) "Removing trace organics by reverse osmosis using cellulose acetate and polyamide membranes", *J. American Water Works Assoc.*, **78**(4),163-174. https://doi.org/10.1002/j.1551-8833.1986.tb05728.x.

Rosa, M.J. and De-Pinho, M.N. (1997), "Membrane surface characterisation by contact angle measurements using the immersed method", *J. Membr. Sci.* **131**, 167-180. PII S0376-

7388(97)00043-4.

Rudra, R., Kumar, V. and Kundu, P.P. (2015), "Acid catalysed cross-linking of poly vinyl alcohol (PVA) by glutaraldehyde: effect of crosslink density on the characteristics of PVA membrane used in single chambered microbial fuel cells", *RSC adv.*, **5**, 83436-83447. https://doi.org/ 10.1039/c5ra16068e.

Seres, Z., Maravic, N., Takaci, A., Nikolic, I., Soronja-Simovic, D., Jokic, A. and Hodur, C. (2016) "Treatment of vegetable oil refinery wastewater using alumina ceramic membrane: optimization using response surface methodology", *J. Clean. Prod.*, **112**, 3132-3137. http://dx.doi.org/10.1016/j.jclepro.2015.10.070.

Sridhar, S., Smitha, B. and Reddy, A.A. (2006), "Separation of 2-butanol–water mixtures by pervaporation through PVA–NYL 66 blend membranes", *Colloids and Surfaces A: Physicochem. Eng. Aspects*, **280**, 95-102. https://doi.org/10.1007/s10853-007-1813-5.

Vasanth, D., Pugalzhenthi, G. and Upaluri, R. (2013), "Crossflow microfiltration of Oil-in-water emulsion using low coast ceramic membrane", *Desal.*, **320**, 86-95. https://doi.org/10.1016/j.desal.2013.04.018.

Wei, J., Qiu, C., Tang, C.Y., Wang, R. and Fane, A.G. (2011), "Synthesis and characterization of flat-sheet thin film composite forward osmosis membranes". *J. Membr. Sci.*, **372**, 292-302. https://doi.org/10.1016/j.memsci.2011.02.013.

Yanilmaz, M., Zhu, J., Lu, Y., Ge, Y. and Zhang, X. (2017) "High-strength, thermally stable nylon 6,6 composite nanofiber separators for lithium-ion batteries", *J. Mater. Sci.*, **52**(9), https://doi.org/10.1007/s10853-017-0764-8.

Zagklis, D.P., Vavouraki, A.I., Kornaros, M.E. and Paraskeva, M.E. (2015), "Purification of olive mill wastewater phenols through membrane filtration and resin adsorption/desorption*", J. Hazard. Mater.*, **285**, 69-76. http://dx.doi.org/10.1016/j.jhazmat.2014.11.038.

Zeng, G.M., Xu, K., Huang, J.H., Li, X., Fang, Y.Y. and Qu, Y.H. (2008), "Micellar enhanced ultrafiltration of phenol in synthetic waste water using polysulfone spiral membrane", *J. Membr. Sci.*, **310**, 149-160. https://doi.org/10.1016/j.memsci.2007.10.046.

CC